

# Rotor Synchronization of Radiofrequency and Gradient Pulses in High-Resolution Magic Angle Spinning NMR

Jean-Michel Wieruszkeski, Gérard Montagne, Gianni Chessari, Pierre Rousselot-Pailley, and Guy Lippens<sup>1</sup>

UMR 8525 CNRS, Institut de Biologie de Lille, Institut Pasteur de Lille, Université de Lille II, 1 rue du Professeur Calmette,  
B.P. 447, 59021 Lille Cedex, France

Received January 16, 2001; revised May 24, 2001

**We have investigated the extent to which rotor synchronization of radiofrequency pulses leads to spectral improvement in high-resolution magic angle spinning NMR experiments. Several pulse sequences were tested, and the effect was found to be maximal in homonuclear TOCSY spectra. The physicochemical nature of the sample plays a role in the phenomenon, as rotor synchronization allows the refocusing of residual anisotropic interactions. However, even in a liquid sample the effects were visible. Radial inhomogeneities of the radiofrequency field were identified as an important source of the problem.** © 2001 Academic Press

**Key Words:** high-resolution magic angle spinning; rotor synchronization; TOCSY; solid-phase synthesis.

## INTRODUCTION

Liquid- and solid-state spectroscopies, traditionally distinguished by the presence or absence of averaged dipolar and chemical-shift anisotropic interactions, have recently converged in a number of studies where the averaging is present but not fully complete. One domain of particular interest to the solid-phase organic chemistry (SPOC) community is the technique of high-resolution magic angle spinning NMR (HR MAS NMR), where appropriate swelling conditions combined with MAS lead to high-resolution spectra (1). The technique applies the pulse sequences of liquid-state spectroscopy to molecular entities that despite their anchoring to a solid phase have liquid-like properties when the resin is well solvated. The fast rotation of the macroscopic sample around the magic angle (2), nowadays used routinely in solid-state NMR, serves here to average out to zero both the inhomogeneities of the magnetic susceptibility and the residual terms of both anisotropic interactions stemming from a nonuniform sampling of the solid angle. The nature of the samples that have been studied by the HRMAS NMR technique varies from pure isotropic liquids over solvent-swollen SPOC resins with a gel-like character to macroscopic solid supports grafted with a more mobile phase. In a liquid sample,

solid-state effects should be completely absent, as molecular tumbling of the peptide in solution represents a completely isotropic situation at the relevant time scale of the rotor period. For the tethered peptides, however, true solid-state effects might become more pronounced, with associated problems of anisotropic interactions that become modulated by the rotation.

Despite the similarity to classical liquid-state spectroscopy, the actions of a number of NMR parameters such as radiofrequency (RF) and gradient pulses with their associated imperfections will be equally modulated over time by the rotation in the HR MAS experiment. That this potentially can lead to artifacts and subsequent spectral degradation has been observed independently by different groups. The TOCSY spectrum of a scorpion toxin solution in a nano-probe required the use of adiabatic pulses during the isotropic mixing time (3). We observed in our study of resin-bound polyalanine peptides (4) that use of the clean-TOCSY sequence led to important artifacts, and a destructive interference between spinning rate and RF pulses in a TOCSY experiment was reported for a resin-bound peptide (5). Very recently, while working with macroscopic solid supports such as the lanterns used for combinatorial chemistry (6), we also noted problems with heteronuclear <sup>1</sup>H–<sup>13</sup>C spectra, especially when we implemented the inverse detection sequences to measure <sup>13</sup>C T<sub>2</sub> relaxation rates (unpublished results).

The aim of the present paper is to investigate the extent to which rotor synchronization of both RF and gradient pulses, a common practice in solid-state NMR, leads to spectral improvement in HR MAS NMR experiments. The pulse sequences into which we introduced rotor synchronization are the LED sequence (7), of great use for solvent suppression in HR MAS NMR (8), the clean-TOCSY sequence (9), and finally the refocused <sup>1</sup>H–<sup>13</sup>C HSQC spectrum (10) which uses a double INEPT period (11) to transfer proton to carbon magnetization and vice versa. To investigate the importance of nonaveraged anisotropic interactions reflecting the physicochemical nature of the sample, we studied the same GlyPheAla tripeptide, first dissolved as a free peptide in DMF, and then grafted onto a polystyrene resin or tethered to the surface of a solid-phase lantern.

<sup>1</sup> To whom correspondence should be addressed.



## MATERIAL AND METHODS

### Synthesis

The tripeptide AlaPheGly was manually synthesized on different solid supports (Rink amide polystyrene resin, *p*-Aminomethyl-polystyrene resin (LCC-Dynospheres), and a Mimotope lanterns) according to the solid-phase method using the Fmoc strategy.

*a. Synthesis of AlaGlyPhe.* The amount of 833 mg (0.5 mmol) of Fmoc-Rink amide resin was used for the synthesis of the peptide AlaPheGly. The resin carrying the peptide was treated for 2 h with a scavenger solution of 95% (v/v) trifluoroacetic acid (TFA), 2.5% (v/v) water, 2.5% (v/v) triisopropylsilane (TIS) in order to cleave the tripeptide from the solid support. The cleaved peptide was precipitated in cold *tert*-butyl methyl ether, lyophilized, and purified by HPLC to obtain 100 mg (68% yield) of solid white powder.

*b. Synthesis of AlaGlyPhe-LCC-Dynospheres.* The peptide AlaPheGly was synthesized using the general procedure on 150 mg (0.29 mmol) of Dynospheres *p*-aminomethyl-

polystyrene resin carrying a nominal charge of 1.95 mmol/g. After the synthesis half of the resin was treated with a solution of 20% TFA in dichloromethane (DCM) for 10 min and then washed extensively with DCM and dried under vacuum conditions for 1 day. This procedure allowed us to have the N terminal of the peptide in the protonated form with trifluoroacetate as counterion.

*c. Synthesis of AlaGlyPhe-lantern.* One lantern functionalized with Fmoc Rink amide linker (35  $\mu$ mol) was treated with a solution of piperidine in DMF (20% v/v) for 20 min in order to remove the Fmoc protecting group. The tripeptide was then synthesized on the unprotected lantern using the general procedure. One-fourth of the functionalized lantern was treated with a minimum quantity of TFA solution (1% TFA in DCM) for 5 min in order to obtain the peptide in the charged form while avoiding any cleavage. The lantern was then washed and dried under vacuum conditions.

### NMR Spectroscopy

The liquid sample was prepared by introducing 100  $\mu$ l of a 30 mM solution of peptide in fully deuterated DMF into a

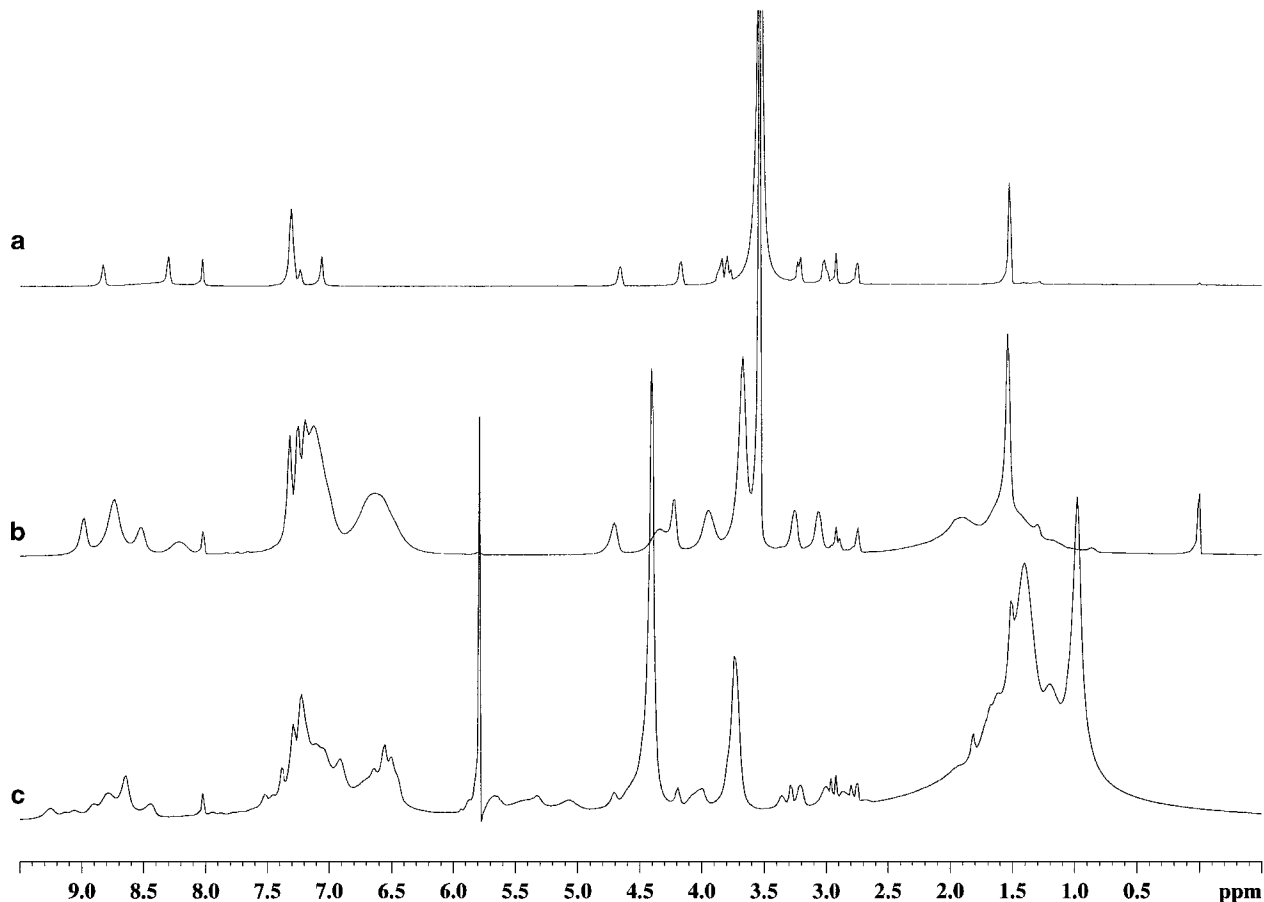


**FIG. 1.** One-dimensional spectra of the three systems under study: (a) the free GlyPheAla peptide, (b) the same peptide grafted onto a polystyrene resin, and (c) grafted onto a solid phase lantern. In the latter sample, the peptide was only partially protonated.

standard 4 mm HR MAS rotor. The resin sample was prepared by introducing 10 mg of dry Dynospheres into the rotor, and by *in situ* swelling with deuterated DMF. For the last sample, one-quarter of lantern was split off manually and introduced into a full rotor. After filling with DMF, the rotor was closed.

All spectra were run on a Bruker DMX 600-MHz spectrometer using a dual  $^1\text{H}$ - $^{13}\text{C}$  HR MAS probe equipped with a self-shielded magnetic field gradient along the magic angle. Pulse lengths at full power were  $9.1\ \mu\text{s}$  for the proton  $90^\circ$  pulse, and  $6.5\ \mu\text{s}$  for the  $^{13}\text{C}$   $90^\circ$  pulse. Details of the different delays used are given in the legend of Fig. 2. One-dimensional spectra were recorded with 64 scans and 2k complex points for a 6000-Hz spectral window, and 2D TOCSY spectra with 16 scans and 2k points during acquisition and 400 complex points in the indirect dimension. The  $^1\text{H}$ - $^{13}\text{C}$  HSQC spectrum was recorded with 32 scans, 2k points in the acquisition, and 400 complex points for again 6000 Hz (40 ppm) in the  $^{13}\text{C}$  dimension. Rotor synchronization was not ensured by a trigger on the rotor position but only by the stable rotation of the sample. Absence of matching of the  $B_1$  fields and the rotation rates was attained by simply changing the rotation rate setting.

## RESULTS

In Fig. 1, we show the 1D spectra of the three samples under study. On the solid-phase lantern, the synthesis occurs through a Rink linker (12), that is cleaved by a concentrated solution of TFA. We treated the lantern with a 1% TFA solution to ensure a charged form ( $\text{NH}^{3+}$ ) for the N terminal Ala residue, but due to the low concentration of TFA used, not all peptide moieties were charged. The double signal for the alanine methyl group reflects both forms, with a 1 ppm chemical shift in the uncharged form and a 1.5 ppm value for the charged peptide. Moreover, the linewidth of the charged form is smaller than for the uncharged one, indicating a lesser mobility for the latter (13).

In order to assess the influence of the rotor synchronization, we implemented the LED sequence (4) with a delay between the pairs of  $90^\circ$  pulses during which the gradient pulse is delivered equal to an integer number of the rotor period at a 6-kHz spinning rate (Fig. 2a). Both the diffusion period and the relaxation delay were equally defined as multiples of the rotor period, and the spectral window was set to 6 kHz or 10 ppm on our spectrometer operating at 600-MHz proton frequency. In order not to change any NMR parameter, the same experiment was run at 6 and 4.5 kHz. In Fig. 3, the LED spectra of the tethered molecules show that resonances of freely diffusing molecules such as the residual protons on the DMF- $d_7$  solvent as well as the broad signals of the matrix are efficiently suppressed, through diffusing filtering for the solvent and  $T_2$  relaxation during the gradient delays, respectively. Synchronization of the various delays leads to a small but reproducible increase in signal intensity, that we estimated to 10–15% depending on the selected resonance. To eliminate the increase in rotation speed as the factor that leads to

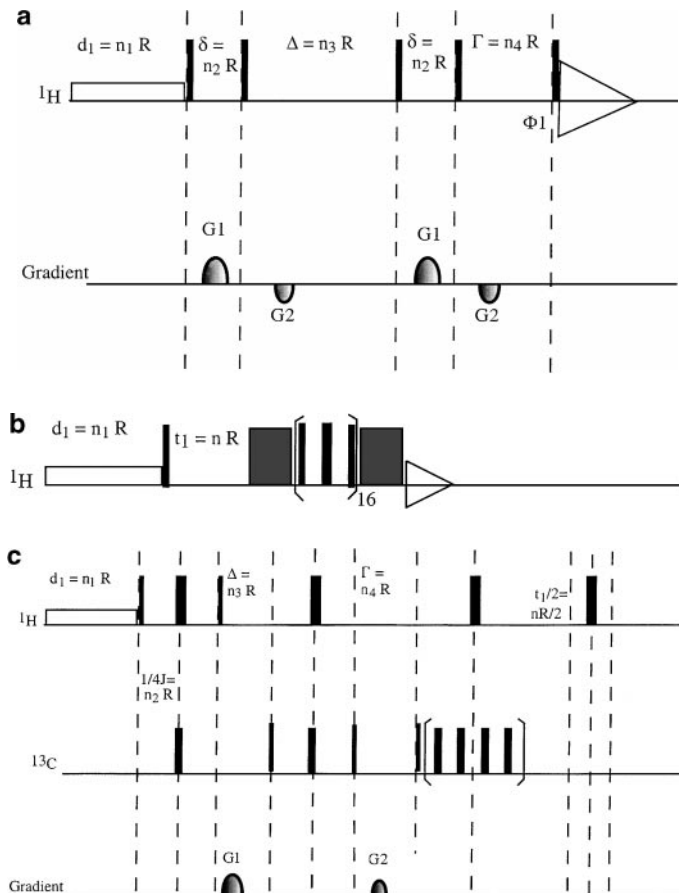


**FIG. 2.** Pulse sequences used are (a) the LED sequence, (b) the clean-TOCSY sequence, and (c) the refocused HSQC with CPMG sequence. Rotor synchronization for the proton acquisition was assured for the 6-kHz spinning rate (corresponding to a rotor period  $R$  of  $166.67\ \mu\text{s}$ ) by using a dwell time equal to  $R$ . (a) In the LED sequence, we used a 1-s relaxation delay ( $n_1 = 600$ ), the G1 and G2 gradients were applied during 5 ms at 30 G/cm and  $500\ \mu\text{s}$  at  $-7\ \text{G/cm}$ , respectively. With the  $500\text{-}\mu\text{s}$  recovery delay, this leads to  $n_2 = 34$  and  $n_4 = 90$ . The total diffusion delay was equal to 34.5 ms, or  $n_3 = 207$ . (b) The clean-TOCSY experiment was set up with a 6-kHz spectral window in both dimensions. The MLEV 16 mixing time was an integer number of the basic cycle, consisting itself of 16 repeats of  $\pi/2$ - $\delta$ - $\pi$ - $\delta$ - $\pi/2$  pulses, where the delay  $\delta$  is equal to the length of the  $\pi$  pulse. With a 12-kHz field strength for the  $B_1$  field, the whole element fits perfectly into one rotor period. The trim pulses before and after the MLEV cycle were set to 1 ms or  $6R$ . (c) In the refocused HSQC sequence used for the  $T_2$  measurements, a 3-s relaxation delay was used, the defocusing delays were set to 1.66 ms ( $n_2 = 10$ ), and the G1 and G2 gradients were applied for 1.3 ms at 28 G/cm and 1 ms at 17 G/cm, respectively. With the  $500\text{-}\mu\text{s}$  recovery delay, this leads to  $n_3 = 12$  and  $n_4 = 10$ . The repetitive element of the CPMG sequence consists of  $\pi$  pulses separated by 4 rotation periods, where proton decoupling is effected by a proton  $\pi$  pulse every fourth  $^{13}\text{C}$  pulse. The  $T_1$  increments are defined as multiples of the rotation period  $R$ , separated in the middle by a proton  $\pi$  pulse that itself is centered in a rotor period. The back-transfer INEPT elements are not shown, as they are synchronized in exactly the same way.

a better averaging of the anisotropic interactions, we performed the experiment again at 7.5 kHz. The resulting intensities being lower than the equivalent ones at 6 kHz demonstrate clearly that synchronization is the determining factor. On the lantern, we

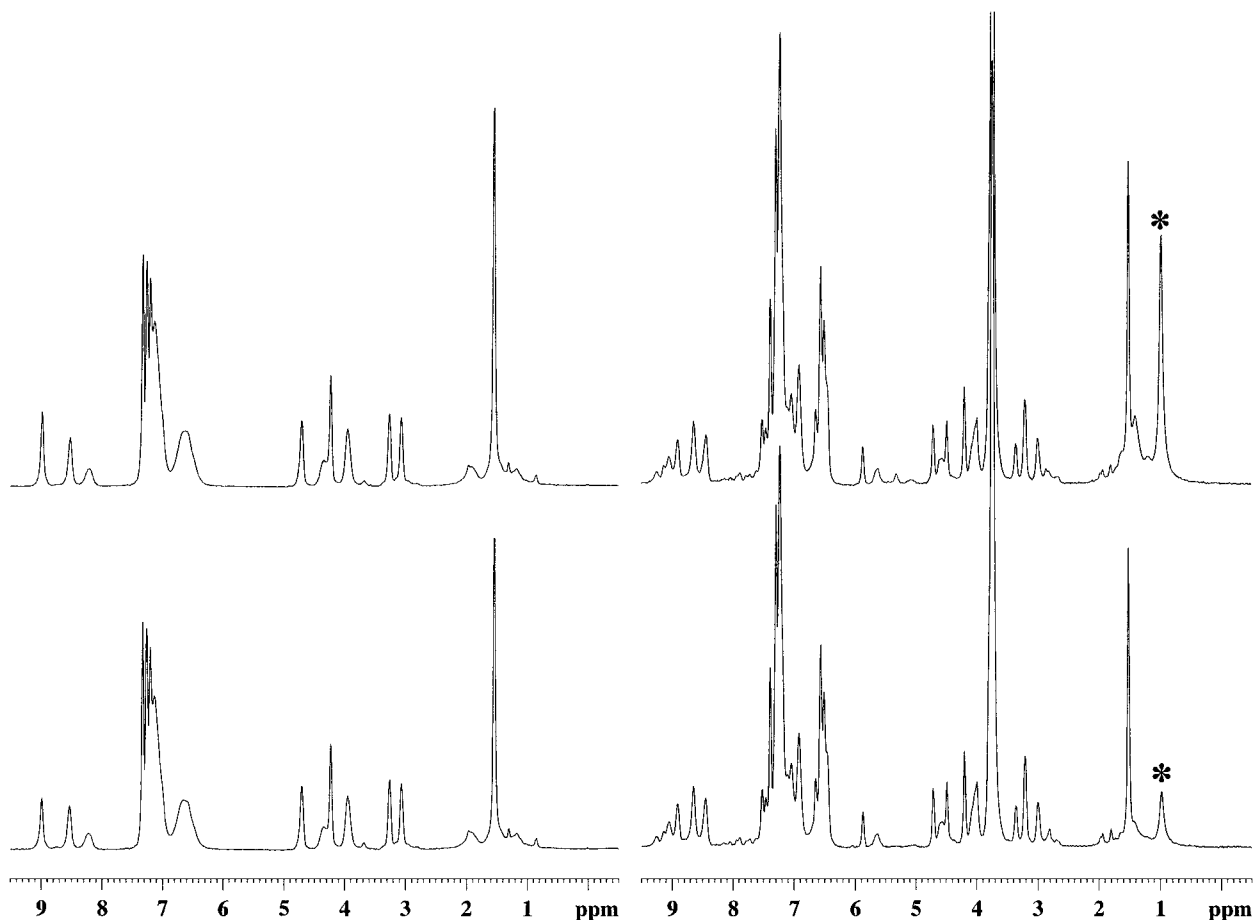


**FIG. 3.** 1D diffusion filtered spectra of the two grafted samples with (top) and without (bottom) rotor synchronization. The \* indicates the methyl proton resonance of the N-terminal Ala residue in the uncharged peptide, for which rotor synchronization leads to a dramatic increase in signal intensity.

found similar factors around 10% for all resonances, except for the last Ala residue in the  $\text{NH}_2$  form, characterized by a 360% increase in signal intensity for the methyl protons.

In the clean-TOCSY experiment, where the mixing sequence performs multiple cycles of the same magnetization transfer from the  $xy$  plane to the  $z$  axis and forth, the effect was found to be seriously enhanced. In Fig. 4, we compare the 1D version of the homonuclear TOCSY sequence on the three samples, run at both 6 and 4.5 kHz. The mixing time of 53 ms consists of 20 loops of a MLEV 16 sequence, where we applied a 12-kHz RF field to ensure rotor synchronization when turning at 6 kHz (Fig. 2b). Both trim pulses before and after the mixing time were defined as a multiple of the rotor period. Already in the first scan, it is clear that synchronization leads to a spectacular improvement of spectral quality. However, whereas in the liquid and the swollen resin samples the first increment still yields some spectral intensity, the 1D clean-TOCSY spectrum of the lantern cannot be interpreted anymore. The situation in the 2D spectra is even more dramatic: synchronization turns the low  $S/N$  and impossible phasing of the 2D spectra into high  $S/N$  and easily phased homonuclear maps (Fig. 5). On the resin

sample, we tried equally the classical TOCSY sequence where no compensation for laboratory and rotating frame relaxation is introduced during the mixing time. In agreement with our previous results on polyalanine (3), the MLEV mixing sequence with the same 12-kHz  $B_1$  field but at 4.5 kHz spinning proved to be far less sensitive to synchronization, although the spectra were of lesser quality than the synchronized clean-TOCSY spectrum.

While running a series of heteronuclear relaxation experiments to evaluate the mobility of the peptides on the lanterns, we noted the low signal to noise ratio of most spectra. Part of the problem was traced back to the purge delays where the coherences are stored (as  $IzSz$  or  $Sz$ ) along the  $z$  axis and a gradient pulse is applied to destroy all coherences that keep a  $x$  or  $y$  component. Synchronization of these sequences was effected for the  $J$  coupling defocusing and refocusing delays, for the purge delays (4 in the refocused HSQC spectrum), for the acquisition times in both dimensions, and finally for the relaxation delay (Fig. 2c). In Fig. 6, we show traces through the HSQC spectra at 6 or 4.5 kHz, and note again the increase in signal upon synchronization.

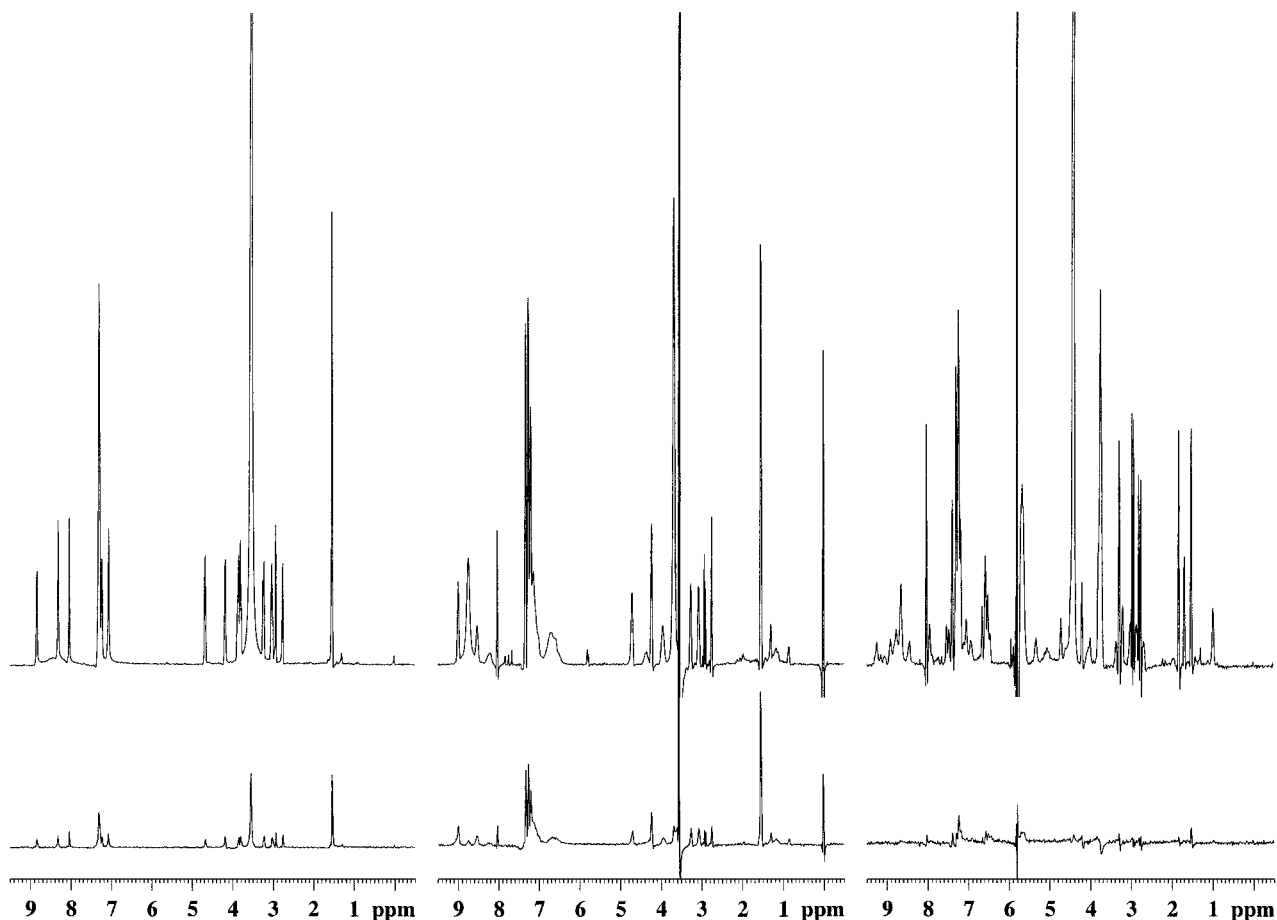


**FIG. 4.** First increment of the homonuclear clean-TOCSY sequence on the three samples, run at both 6 kHz (top) and 4.5 kHz (bottom). The mixing time was 53.3 ms corresponding to 20 cycles of the MLEV 16 train.

## DISCUSSION

In many cases, liquid-state NMR spectroscopy pulse sequences flip magnetization from the  $xy$  plane to the  $z$  axis and forth. This is the case in the LED sequence (7), where magnetization storage along the  $z$  axis during the diffusion delay leads to  $T_1$  rather than  $T_2$  relaxation, in the clean-TOCSY mixing time where the opposite sign of laboratory and rotation frame cross-relaxation is used to promote magnetization transfer uniquely by  $J$  coupling without cross-relaxation (9), and in the HSQC sequence where a gradient pulse destroys both terms of non- $^{13}\text{C}$ -linked protons and magnetization components that due to differential  $J$  couplings or pulse imperfections has not evolved perfectly in anti-phase terms (14). In all of these cases, pulse imperfections have only a mild effect, as they are immediately compensated by the following pulse with the same imperfections but opposite phase. The crucial conditions to achieve compensation, however, is that the imperfection is reproducible over time. A RF amplitude locally inferior to the nominal strength, for example, will lead to a less than  $90^\circ$  pulse, but the pulse restoring the magnetization will also be less than  $90^\circ$  and therefore

compensate the initial missetting. The same is true for other regions of the sample, where the field strength might be superior to the nominal strength. Under rapid spinning conditions such as encountered in the case of MAS, however, potential problems can arise from the coupling between imperfections and movement. In the same example of RF strength as given above, a given spin might experience a less than  $90^\circ$  pulse at a certain moment, because at the absolute position where it is, the field strength is too low, whereas it might be at the location of too high a field strength when the restoring pulse is given. The pulse imperfections therefore will not necessarily be balanced, resulting in a net signal decrease. A recent report attributed these pulse imperfections to the fact that a solenoid coil cannot be made perfectly  $B_1$  homogeneous in its radial plane, due to the asymmetry in its wiring (15), and confirmed with numerical calculations based on a sum of cosine modulations that 10%  $B_1$  inhomogeneity might lead to the observed spectral degradation. The sum of cosine modulations was required to explain the presence of spectral artifacts not only when two MLEV cycles were fitted into one rotor period, but also for other frequencies such as the 4.5 kHz that we used for our experiments.

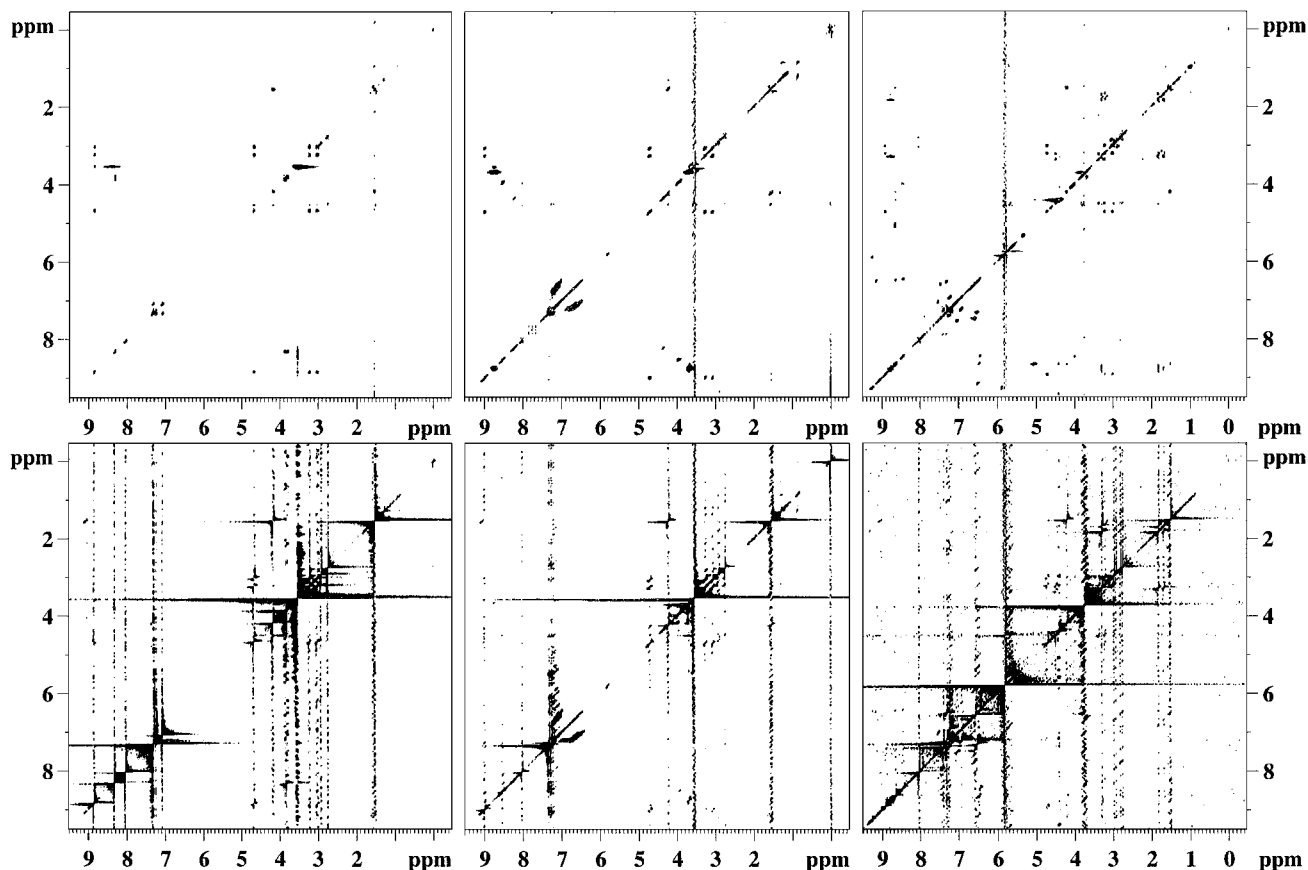


FIG. 5. Two-dimensional homonuclear clean-TOCSY sequence on the three samples, run at both 6 kHz (top) and 4.5 kHz (bottom).

The LED sequence and the refocused HSQC both contain a limited number of periods during which magnetization is stored along the  $z$  axis before being flipped back in the  $xy$  plane, and gains with rotor synchronization, although easily detectable, proved to be not that important. For the liquid sample, where the diffusion-filtered experiment could not be implemented under the same conditions as those for the solid supports, the traces through the HSQC spectra indicated a signal gain of 12% upon synchronization. Similar values were found when the LED sequence or the refocused HSQC was applied to the resin sample, confirming the liquid-like behavior of the tethered molecules. Moreover, the effect proved to be similar when we spun the sample at 7.5 kHz, excluding the increased speed of rotation as the primary source of signal improvement.

The situation was severely amplified in the case of the clean-TOCSY sequence, where the flip-back pulse pairs are repeated numerous times. Amazingly, for both liquid- and resin-bound samples, the absence of synchronization led to unphasable 2D maps. The regular TOCSY sequence without the laboratory frame relaxation delays separating the pulses in the MLEV sequence proved to be less sensitive to rotor synchronization, probably because of the lesser separation and subsequent better compensation of following pulses. Still, upon consideration of

the traces through the synchronized clean-TOCSY and regular MLEV sequence, the former led to a higher quality spectrum and remains therefore preferable.

In order to further explore our initial hypothesis of  $B_1$  inhomogeneity, a regular sample consisting of 3 mg of resin was compared with a sample containing a limited number of swollen beads in a capillary tube centered on the rotor axis (Fig. 7). Two clean-TOCSY cycles led to a more significant signal decrease for the full sample than for the concentric one, when we changed the rotation rate from 6 to 3 kHz. More specifically, for the  $H\alpha$  proton of the Phe residue, we found for the full rotor a factor of 0.18 between the signals at 6 and 3 kHz, and a factor of 0.34 for the concentric one. The results were similar for the residual DMF signals. Amazingly, when we used the same samples on a 300 MHz spectrometer, while using the same  $B_1$  field of 12 kHz, rotor synchronization proved to be less important, as we found factors of 0.3 and 0.45 for the full or concentric sample upon changing the rotation rate from 6 to 3 kHz. Therefore, the wavelength of the electromagnetic radiation itself also seems to play a role in the phenomenon.

For the lantern, the fact of synchronizing the LED or HSQC intervals led to the highest signal increase for the N-terminal alanine residue in the  $NH_2$  form. Because we have indications

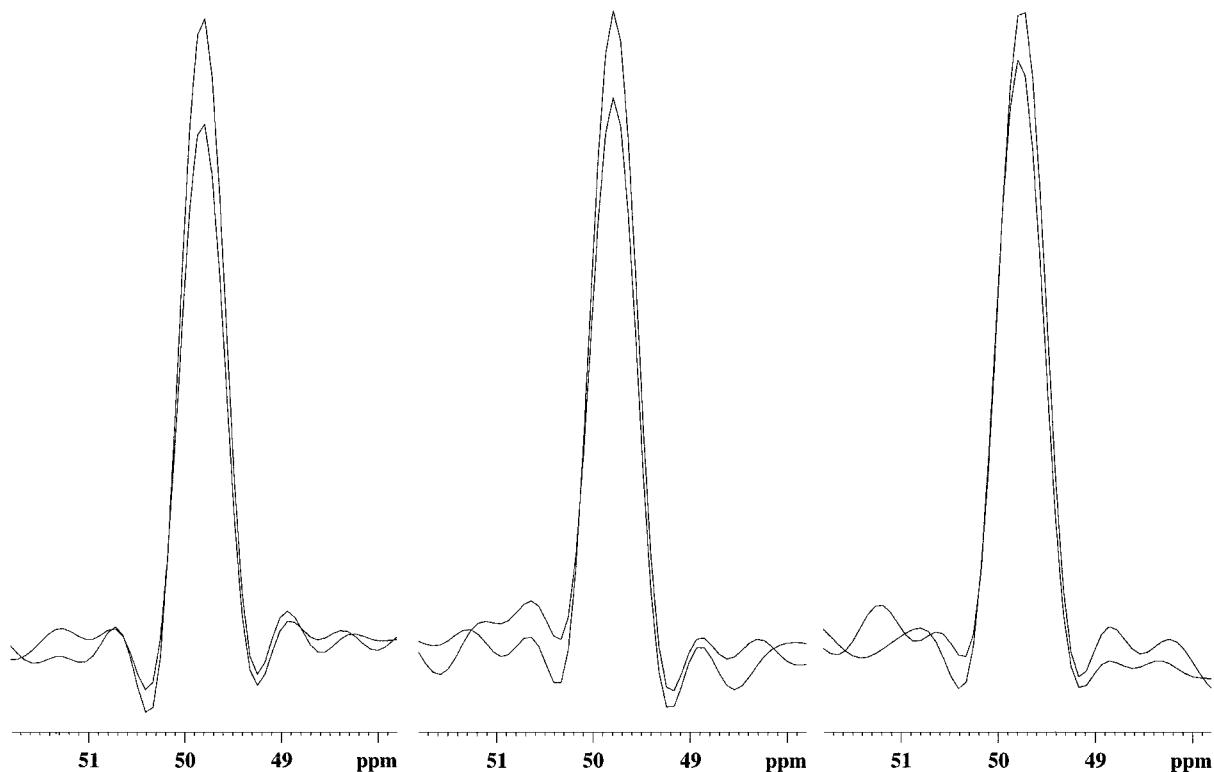


**FIG. 6.** Trace through the  $H\alpha$ - $C\alpha$  resonance of Phe of the three samples in the two-dimensional heteronuclear refocused HSQC sequence with a CPMG spin-lock period of 2.6 ms, run at both 6 kHz (top) and 4.5 kHz (bottom).

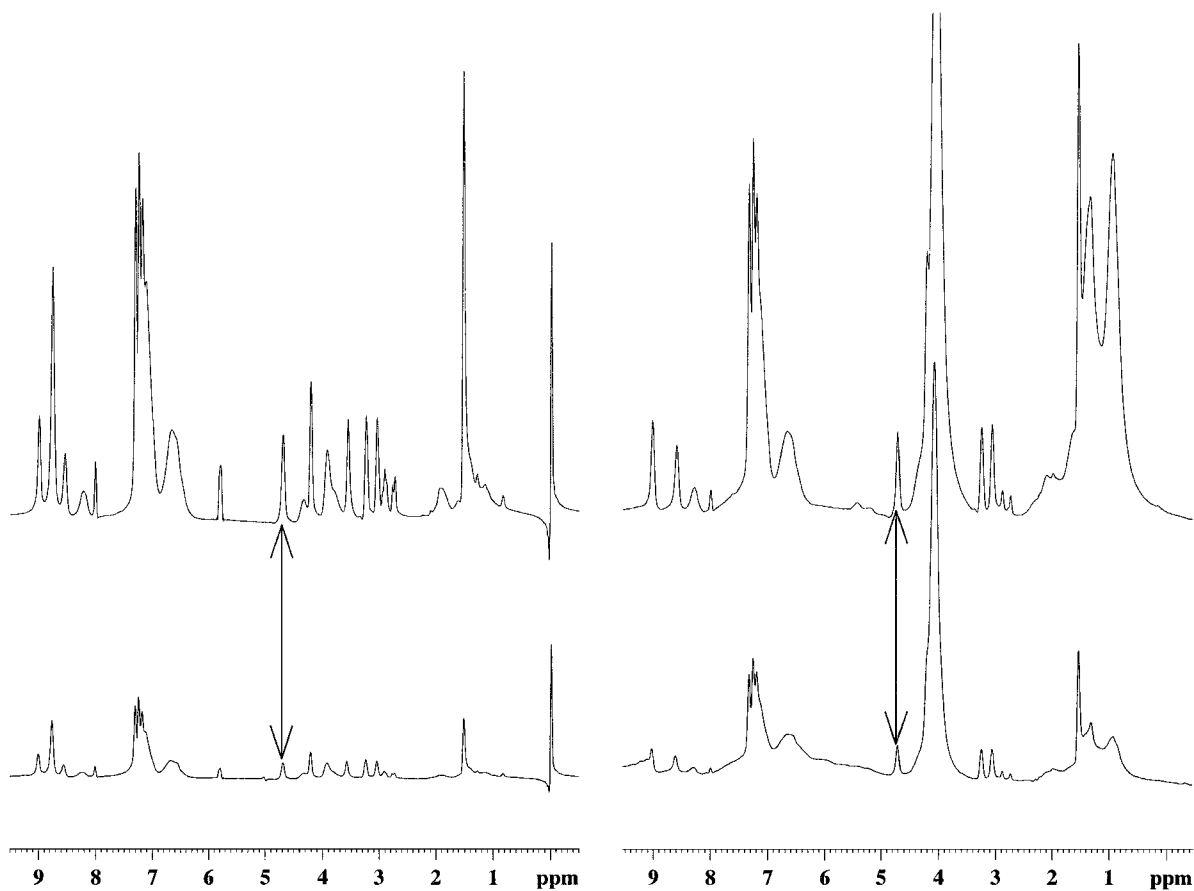


**FIG. 7.** Homonuclear one-dimensional clean-TOCSY sequence on a resin sample in a full rotor (left) or concentric one (right), at 6 kHz (top) and 3 kHz (bottom). The mixing time was 5 ms corresponding to 2 cycles of the MLEV16 train. The solid arrow indicates the Phe- $H\alpha$  signal whose intensity loss was used to quantify the effect.

that this residue is less mobile, we believe that beyond the modulation of pulse imperfections, the physicochemical nature of the sample does couple to the rotation leading to spectral deterioration. When the magnetization associated with a truly solid sample is in the  $xy$  plane, the evolution of the density matrix under the second order anisotropic components of the Hamiltonian is exactly averaged to zero after every rotor period, leading to a refocusing of all individual spin vectors. Moreover, omitting rotor synchronization of a mixing time during which  $z$  magnetization is present, such as in a chemical exchange experiment, leads to off-diagonal side bands even without a molecular exchange process and complicates the generation of absorptive side bands in the spectrum (16). For the lantern-grafted peptide, where at least the plastic support is a true solid, the residual anisotropic terms might contribute to similar artifacts that can only be alleviated by rotor synchronization. This is particularly evident for the methyl protons of the N-terminal Ala residue grafted on the lantern, where the large signal loss during the nonsynchronized LED or HSQC sequence most probably finds its origin in the nonaveraged anisotropic interactions with the solid support.

Finally, it should be stressed that our experimental procedure only guarantees rotor synchronization within a single scan. Indeed, as we do not trigger on a rotor position to start a scan, small oscillations in the spinning speed (stable at  $\pm 5$  Hz on our system) make that the synchronization over the whole experiment is not fulfilled. Still, we think that the above described modulations of pulse imperfections and possible solid-state effects are well compensated by the simple procedure of ensuring that a given spin feels two flip-back pulses at the same absolute location in space, which can easily be done with the existing hardware.

## CONCLUSION

We have shown for three samples of the same tripeptide, free in solution and anchored to a resin or lantern, that rotor synchronization of pulses can lead to a significant improvement of spectral quality. The effect is ascribed partially to pulse imperfections that are modulated over time and is therefore the most severe in pulse sequence such as the clean-TOCSY where multiple pulse trains are delivered during the mixing time. Solid-state

effects also can equally play a role for samples with a more pronounced solid character, such that in those samples even more important gains can be expected from our simple procedure.

## REFERENCES

1. (a) W. L. Fitch, G. Detre, C. P. Holmes, J. N. Shoorely, and P. A. Keifer, *J. Org. Chem.* **59**, 7955 (1994); (b) R. C. Anderson, J. P. Stokes, and M. J. Shapiro, *Tetrahedron Lett.* **36**, 5311 (1995); (c) R. C. Anderson, M. A. Jarema, and M. J. Shapiro, J. P. Stokes, and M. J. Zilix, *J. Org. Chem.* **60**, 2650 (1995); (d) P. A. Keifer, *J. Org. Chem.* **61**, 1558 (1996); (e) C. Dhalluin, I. Pop, B. Depréz, P. Melnyk, A. Tartar, and G. Lippens, ACS Symposium Series, "Molecular Diversity and Combinatorial Chemistry" (K. Janda, Ed.), Am. Chem. Soc., Washington, DC (1996); (f) A. M. Nechifor, A. P. Philipse, F. de Jong, J. P. M. van Duynhoven, R. J. M. Egberink, and D. N. Reinhoudt, *Langmuir* **12**, 3844 (1996).
2. (a) I. J. Lowe, *Phys. Rev. Lett.* **2**, 285 (1959); (b) E. R. Andrew, A. Bradbury, and R. G. Eades, *Nature* **182**, 1659 (1958).
3. M. Delepierre, A. Prochnika-Chalufour, and L. D. Possani, *Biochemistry* **36**, 2649 (1997).
4. R. Warrass, J.-M. Wieruszski, C. Boutillon, and G. Lippens, *J. Am. Chem. Soc.* **122**, 1789 (2000).
5. K. Elbayed, J. Furrer, J. Raya, J. Hirschinger, M. Piotto, M. Bourdonneau, A. Bianco, G. Guichard, D. Limal, and J.-P. Briand, European Peptide Symposium, Montpellier, France, September 2000, Poster 220.
6. F. Rasoul, F. Ercole, Y. Pham, C. T. Bui, Z. Wu, S. N. James, R. W. Trainor, G. Wickham, and N. Maeji, *J. Biopolymers (Pept. Sci.)* **55**, 207 (2000).
7. (a) S. J. Gibbs and C. S. Johnson, *J. Magn. Reson.* **93**, 395 (1991); (b) A. S. Altieri, D. P. Hinton, and R. A. Byrd, *J. Am. Chem. Soc.* **117**, 7566 (1995).
8. R. Warrass, J.-M. Wieruszski, and G. Lippens, *J. Am. Chem. Soc.* **121**, 3787 (1999).
9. C. Griesinger, G. Otting, K. Wüthrich, and R. R. Ernst, *J. Am. Chem. Soc.* **110**, 7870 (1988).
10. D. A. Vidusek, M. F. Roberts, and G. Bodenhausen, *J. Am. Chem. Soc.* **104**, 5452 (1982).
11. G. A. Morris and R. J. Freeman, *J. Am. Chem. Soc.* **101**, 760 (1979).
12. H. Rink, *Tetrahedron Lett.* **28**, 3787 (1987).
13. G. Chessari, J.-M. Wieruszski, and G. Lippens, European Peptide Symposium, Montpellier, France, September 2000, Poster 218.
14. S. Mori, C. Abeygunawardan, M. O'Neil Johnson, and P. C. M. van Zijl, *J. Magn. Reson. B* **108**, 94 (1995).
15. M. Piotto, M. Bourdonneau, J. Furrer, A. Bianco, J. Raya, and K. Elbayed, *J. Magn. Reson.* **149**, 114 (2001).
16. A. F. de Jong, A. P. Kentgens, and W. S. Veeman, *Chem. Phys. Lett.* **109**, 337 (1984).